JOURNAL OF VIROLOGY, Mar. 2000, p. 2323–2332 Vol. 74, No. 5
0022-538X/00/$04.00+0

Rotavirus Infection Induces an Increase in Intracellular Calcium Concentration in Human Intestinal Epithelial Cells: Role in Microvillar Actin Alteration

JEAN-PHILIPPE BRUNET, JACQUELINE COTTE-LAFFITTE, CATHERINE LINXE, ANNE-MARIE QUERO, MONIQUE GÉNITEAU-LEGENDRE, AND ALAIN SERVIN*

Institut National de la Santé et de la Recherche Médicale, Unité 510, Pathogènes et Fonctions des Cellules Épithéliales Polarisées, Faculté de Pharmacie, Université Paris XI, 92296 Châtenay-Malabry cedex, France

Received 14 September 1999/Accepted 6 December 1999

Rotaviruses, which infect mature enterocytes of the small intestine, are recognized as the most important cause of viral gastroenteritis in young children. We have previously reported that rotavirus infection induces microvillar F-actin disassembly in human intestinal epithelial Caco-2 cells (N. Jourdan, J. P. Brunet, C. Sapin, A. Blais, J. Cotte-Laffitte, F. Forestier, A. M. Quero, G. Trugnan, and A. L. Servin, J. Virol. 72:7228–7236, 1998). In this study, to determine the mechanism responsible for rotavirus-induced F-actin alteration, we investigated the effect of infection on intracellular calcium concentration ($[Ca^{2+}]_i$) in Caco-2 cells, since Ca^{2+} is known to be a determinant factor for actin cytoskeleton regulation. As measured by quin2 fluorescence, viral replication induced a progressive increase in $[Ca^{2+}]_i$ from 7 h postinfection, which was shown to be necessary and sufficient for microvillar F-actin disassembly. During the first hours of infection, the increase in $[Ca^{2+}]_i$ was related only to an increase in Ca^{2+} permeability of plasmalemma. At a late stage of infection, $[Ca^{2+}]_i$ elevation was due to both extracellular Ca^{2+} influx and Ca^{2+} release from the intracellular organelles, mainly the endoplasmic reticulum (ER). We noted that at this time the $[Ca^{2+}]_i$ increase was partially related to a phospholipase C (PLC)-dependent mechanism, which probably explains the Ca^{2+} release from the ER. We also demonstrated for the first time that viral proteins or peptides, released into culture supernatants of rotavirus-infected Caco-2 cells, induced a transient increase in $[Ca^{2+}]_i$ of uninfected Caco-2 cells, by a PLC-dependent efflux of Ca^{2+} from the ER and by extracellular Ca^{2+} influx. These supernatants induced a Ca^{2+}-dependent microvillar F-actin alteration in uninfected Caco-2 cells, thus participating in rotavirus pathogenesis.

Rotaviruses, members of the *Reoviridae* family, are recognized as the most important cause of viral gastroenteritis in young children and animals. Although much is known about their replication and maturation processes, the pathophysiologic mechanisms by which rotavirus infection induces diarrhea remain unclear. In order to approach in vitro the situation in vivo and gain further insights into the pathophysiologic mechanisms of rotavirus infection, we (19–21) and others (34) have used the human intestinal epithelial cell line Caco-2. These cells, established from a human colon adenocarcinoma (12), spontaneously differentiate after confluency and display many of the morphologic and biochemical properties of mature enterocytes (30, 39). These characteristics include cellular polarization, with the appearance of an apical brush border and the expression of a variety of enterocytic hydrolases. Since rotaviruses have been described to exhibit marked tropism for the differentiated enterocytes of the intestinal epithelium (4, 7), Caco-2 cells currently represent an appropriate model for in vitro studies of rotavirus infection.

We have recently reported that infection of Caco-2 cells with the simian rotavirus strain RRV selectively induces a decrease in the activity and apical expression of the brush border-associated hydrolase sucrase-isomaltase (SI). These alterations have been shown to result from a profound alteration in the intracellular traffic of the enzyme, concomitant with microvillar F-actin and villin disassembly (19). We have hypothesized that cytoskeleton disorganization could be implicated in functional perturbations, such as alteration in apical surface expression of SI, which lead to the default in nutrient digestion and thereby indirectly participate in triggering of diarrhea. However, the mechanisms of apical actin alteration in rotavirus-infected Caco-2 cells remain unknown. Since it is now well documented that Ca^{2+} is a determinant factor for actin cytoskeleton regulation through actin-binding proteins (13, 38), elevation of intracellular calcium concentration ($[Ca^{2+}]_i$) in rotavirus-infected Caco-2 cells may be implicated in the alteration of microvillar actin. Several studies seem to indicate that Ca^{2+} is a determinant factor in rotavirus cytopathogenesis. Michelangeli et al. (27) have shown that rotavirus-specific protein synthesis induces alteration in Ca^{2+} homeostasis in infected MA104 cells. They indicated that the increase in $[Ca^{2+}]_i$ results from an increase of plasma membrane permeability. An increase of the intracellular sequestered Ca^{2+} pools has also been measured (26, 27). The effect of viral protein synthesis on $[Ca^{2+}]_i$ homeostasis may be responsible for cytopathic effect and cell death (26, 29). Tian et al. (35, 36) have reported that the expression of the rotavirus nonstructural protein NSP4 increases $[Ca^{2+}]_i$ in *Spodoptera frugiperda* (Sf9) cells. This elevation in $[Ca^{2+}]_i$ was not due to an increased influx of extracellular Ca^{2+} but seemed to result from the increase in Ca^{2+} efflux from the endoplasmic reticulum (ER) (35). Exogenous application of purified NSP4 or a peptide comprising amino acid residues 114 to 135 of NSP4 also mobilized Ca^{2+} from internal stores in Sf9 cells, but through a phospholipase C (PLC)-dependent mechanism (35). In the human colonic adenocarcinoma cell line HT-29, exogenous NSP4 was shown to induce both Ca^{2+} release from intracellular stores and plas-

* Corresponding author. Mailing address: INSERM U-510, Faculté de Pharmacie, 5 rue J. B. Clément, 92296 Châtenay-Malabry cedex, France. Phone and fax: 33-1 46 83 56 61. E-mail: alain.servin@cep.u-psud.fr.

malemma Ca^{2+} influx, through receptor-mediated PLC activation and inositol 1,4,5-triphosphate (IP_3) production (9). The same laboratory has reported that NSP4 or amino acid residues 114 to 135 of NSP4 induced diarrhea in young mice when injected intraperitoneally or intraileally, confirming the possible role of NSP4 in triggering of diarrhea (2). They proposed that NSP4 could act as a viral enterotoxin. However, Ca^{2+} homeostasis studies conducted in vitro have not allowed simultaneous observation and discrimination of the effects of endogenously expressed viral proteins in infected cells and the effects of extracellular released viral proteins on neighboring cells.

In this work, we investigated Ca^{2+} homeostasis in RRV-infected Caco-2 cells. Our results indicate that viral replication induces $[Ca^{2+}]_i$ increase through an altered Ca^{2+} permeability of plasmalemma and at a late stage of infection also by a PLC-dependent efflux of Ca^{2+} from the ER. We have demonstrated for the first time that viral proteins or peptides released in the culture supernatants at a late stage of rotavirus infection induce a transient increase in $[Ca^{2+}]_i$ of uninfected Caco-2 cells. The $[Ca^{2+}]_i$ increases observed in RRV-infected cells and supernatant-treated uninfected Caco-2 cells both induce microvillar F-actin disassembly. This structural alteration could be an important step in rotavirus pathogenesis, since it could participate in triggering of diarrhea through functional perturbations of enterocytes.

MATERIALS AND METHODS

Reagents. Ionomycin, trypsin, paraformaldehyde, Triton X-100, 1,4-diazabicyclo-(2.2.2.)octane (DABCO), NaCl, KCl, $CaCl_2$, $MgCl_2$, $MnCl_2$, HEPES, 4′-aminomethyl-4,5′,8-trimethylpsoralen, EGTA, and 2,5-di(*tert*-butyl)-1,4-benzohydroquinone (tBuBHQ) were purchased from Sigma. 1,2-bis(2-Aminophenoxy)ethan-*N*,*N*,*N*′,*N*′-tetraacetic acid acetoxymethyl ester (BAPTA-AM) and 2-[(2-amino-5-methylphenoxy)methyl]-6-methoxy-8-aminoquinoline-*N*,*N*,*N*′,*N*′-tetraacetic acid tetraacetoxymethyl ester (quin2-AM) were from Molecular Probes (via Interchim, Montluçon, France). Glycergel and IDEIA rotavirus were from Dako (Dakopatts, Copenhagen, Denmark). D-Glucose, Tween 20, and dimethyl sulfoxide were obtained from Prolabo (Paris, France). U-73122 and U-73343 were purchased from Calbiochem via France Biochem, Meudon, France. Products for cell culture were from Life Technologies, Eragny, France. The bicinchoninic acid assay kit was from Pierce via Interchim.

Cells and culture conditions. The Caco-2 cell line was established from a human colon adenocarcinoma by J. Fogh (12). Caco-2 cells (passages 60 to 90) were grown in Dulbecco's modified Eagle's medium (DMEM; Gibco) supplemented with 15% (vol/vol) heat-inactivated fetal calf serum (FCS), 1% nonessential amino acids, 100 U of penicillin/ml, and 100 μg of streptomycin/ml at 37°C in a humidified 10% CO_2 incubator. Caco-2 cells (10^4/cm^2) were seeded in 25-cm^2 culture flasks (Corning) for intracellular calcium concentration studies and in 24-well plates (TPP) containing coverslips for cytoskeleton studies. The medium was changed every day, and the cells were used for 14 to 16 days after seeding. MA104 cells were grown in MEM supplemented with 10% FCS, 2 mM glutamine, 1% nonessential amino acids, 20 U of penicillin/ml, and 40 U of streptomycin/ml at 37°C in a humidified 5% CO_2 incubator. Cells (10^5/cm^2) were seeded in 150-cm^2 culture flasks (Falcon; Becton Dickinson) for virus stock production and in six-well plates (Falcon, Becton Dickinson) for virus titration. MA104 cells were used 48 h after seeding.

Virus. Rhesus rotavirus RRV was obtained from J. Cohen (Institut National de la Recherche Agronomique, Jouy-en-Josas, France). Virus stocks were generated in MA104 after 24-h preincubation of the cells in serum-free medium. Virus was activated by treatment with trypsin (0.5 μg/ml) at 37°C for 30 min. MA104 cell monolayers were then infected at a multiplicity of infection (MOI) of 0.002. After 1 h of adsorption at 37°C, the inoculum was removed and infected cells were incubated in culture medium containing 0.5 μg of trypsin/ml. After exhibiting a complete cytopathic effect, the cultures were freeze-thawed and cell debris was removed by centrifugation. The titers of virus were determined by plaque assay on MA104 cells as previously described (10).

Virus inactivation. Genetic inactivation of cell culture-derived RRV was accomplished through a process using psoralen and long-wave UV light that irreversibly cross-links viral RNA but does not alter the hemagglutination function or antigenic characteristics of rotavirus proteins (15). Two milliliters of virus suspension was mixed with 4′-aminomethyl-4,5′,8-trimethylpsoralen at 20 μg/ml in a petri box (30-mm diameter) and incubated at 4°C for 15 min. Virus was then exposed to UV light at 366 nm for 40 min. The petri box was placed on ice, and the distance between the surface of the suspension and the light source was 2 cm. The effectiveness of psoralen-UV inactivation was demonstrated by the lack of detectable viral antigen in an immunofluorescence assay in MA104-infected cells with psoralen-UV-treated RRV (data not shown). Inactivated and untreated RRV samples were compared by spectrophotometric A_{260} and A_{280} measurements to ensure that similar viral masses were still present after the inactivation process. An immunoassay with a rabbit polyclonal antibody was used to detect group A-specific proteins, including the major intermediate capsid protein VP6 (IDEIA rotavirus). There was no difference between psoralen-UV-treated and untreated RRV (not shown). A hemagglutination assay was used to provide a measure of the integrity of the VP4 protein on the outer capsid of RRV and thus outer capsid integrity. The titers did not significantly vary between treated and untreated samples (data not shown).

Virus infection of Caco-2 cells. Caco-2 cells, cultured without FCS during 24 h, were infected with an inoculum of trypsin-activated RRV at an MOI of 10 PFU/cell for 1 h at 37°C. The inoculum was then removed, and fresh medium containing 0.5 μg of trypsin/ml was added. This time was taken as time zero for all experiments. Infected cells were incubated at 37°C in a humidified 10% CO_2 incubator and were processed for experiments at the indicated times postinfection (p.i.).

Measurement of cell viability. The lactate dehydrogenase (LDH) activity in the culture medium was assayed by measuring the oxidation of NADH with pyruvate as a substrate at 340 nm with an Enzyline LDH kit (Biomerieux, Paris, France) according to the manufacturer's instructions. Protein was assayed with the bicinchoninic acid assay (Pierce). Results were expressed as milliunits of LDH activity per milligram of protein in cell monolayers.

Determination of $[Ca^{2+}]_i$. The $[Ca^{2+}]_i$ was measured using the fluorescent indicator quin2, which was incorporated intracellularly as its acetoxymethyl ester quin2-AM. Quin2-AM was chosen in preference to fura2 because of less compartmentalization of this dye within membrane-bound cytoplasmic organelles in Caco-2 cells. Stock quin2-AM was dissolved in 100% dimethyl sulfoxide to a concentration of 1 mg/ml and stored at −20°C. Cell monolayers were trypsinized, washed twice in serum-free DMEM by centrifugation, and resuspended in serum-free DMEM at a concentration of 1.5×10^6 cells per ml. The cells were incubated in the dark with 50 μM quin2-AM for 30 min at 37°C. After loading, to remove extracellular quin2-AM, cells were washed twice by centrifugation in an extracellular medium (EM) containing 116 mM NaCl, 1.2 mM KCl, 1.2 mM $MgCl_2$, 1.8 mM $CaCl_2$, 10 mM HEPES, and 1 g of glucose/liter (pH 7.4). The cells were resuspended to 1.5×10^6 cells per ml and incubated for 45 min in the dark, at room temperature, to allow for maximum dye deesterification. For all measurements, cells were temperature equilibrated in a thermostatically controlled quartz cuvette (37°C) equipped with a magnetic microstirrer. Fluorescence was measured in a Perkin-Elmer LS-50 spectrofluorimeter with the excitation and emission wavelengths being recorded at 339 and 492 nm, respectively. $[Ca^{2+}]_i$ was evaluated by the method of Tsien et al. (37), using an equilibrium dissociation constant (K_d) for the quin2-Ca^{2+} complex at 37°C of 115 nM. Calibration was performed for each sample after the sequential addition of Triton X-100 and then 25 mM EGTA to the cell suspension to provide the respective maximum (F_{max}) and minimum (F_{min}) fluorescence. $[Ca^{2+}]_i$ (nanomolar) was calculated as $K_d[(F - F_{min})/(F_{max} - F)]$. Autofluorescence was constant throughout each measurement and did not affect calculation of $[Ca^{2+}]_i$.

Assessment of membrane Ca^{2+} permeability. (i) Step change in extracellular Ca^{2+} concentration. The relative Ca^{2+} permeability of control and virus-infected cells was evaluated by imposing a step increase in the extracellular Ca^{2+} concentration and measuring the rate of change in $[Ca^{2+}]_i$ during the first few seconds. This change is the result of the net Ca^{2+} flux between the cytoplasm and the external medium and between the cytoplasm and Ca^{2+}-sequestering organelles. Nevertheless, the elevation in $[Ca^{2+}]_i$ during the first few seconds should be a measurement of unidirectional Ca^{2+} flux and therefore of calcium permeability.

(ii) Mn^{2+} influx. Mn^{2+} enters epithelial cells by the same route as Ca^{2+} (24, 25). The rate of quenching of quin2 fluorescence by Mn^{2+} was used to estimate plasma membrane permeability to Ca^{2+} and the effect of rotavirus infection on this parameter (27). The measurements were made at excitation and emission wavelengths of 366 nm and 492 nm, respectively, wavelengths at which quin2 fluorescence is independent of Ca^{2+} concentration (16). We normalized the fluorescence to the initial intensity just before the addition of Mn^{2+} (100%). Triton X-100 was added to obtain the fully quenched value, which was taken as basal (0%). The slope was related to the membrane permeability to Mn^{2+} and, hence, Ca^{2+}.

Measurement of stored Ca^{2+} pools. Ionomycin, a Ca^{2+} ionophore, was used to release Ca^{2+} from the internal stores including the ER, the mitochondria, and other intracellular organelles. Ionomycin transports Ca^{2+} across the plasma membrane and the intracellular organelle membranes. In the absence of extracellular Ca^{2+}, the rise in $[Ca^{2+}]_i$ induced by ionomycin was used as an index of Ca^{2+} released from the total internal Ca^{2+} pool. Quin2-AM-loaded Caco-2 cells were washed twice in Ca^{2+}-free EM containing 100 μM EGTA and resuspended in this buffer immediately before fluorescence measurement. At various times after suspension of the cells in Ca^{2+}-free EM, 5 μM ionomycin was added and the $[Ca^{2+}]_i$ was measured as previously described.

Measurement of Ca^{2+} release from ER. The ER membrane has channels that release Ca^{2+} into the cytoplasm. A Ca^{2+}-ATPase pump in the ER membrane transports Ca^{2+} from the cytoplasm back to the ER. When the Ca^{2+}-ATPase pump in the ER is inhibited by the specific inhibitor tBuBHQ (17, 22), Ca^{2+} that

leaks from the ER is not resequestered by the pumps resulting in depletion of the ER stores. Fifty micromolar (final concentration) tBuBHQ was added to cells 1 h before trypsinization and quin2-AM loading. The time of tBuBHQ addition was chosen to avoid any interference with virus replication.

Effects of culture supernatants of RRV-infected Caco-2 cells on $[Ca^{2+}]_i$. After indicated times of infection, culture supernatants of RRV-infected cells were collected and 1 ml was added directly in the spectrofluorimeter cuvette to 2×10^6 quin2-AM-loaded uninfected Caco-2 cells for $[Ca^{2+}]_i$ measurements. In all experiments, the addition of supernatants corresponded to time zero. To determine if proteins are involved in the effects of supernatants on $[Ca^{2+}]_i$, supernatants of infected cells were incubated at 95°C during 5 min to induce protein denaturation. Heated supernatants were added to 2×10^6 quin2-AM loaded cells for $[Ca^{2+}]_i$ measurements. To determine if the increase in $[Ca^{2+}]_i$ induced by supernatants of infected cells was dependent on cellular or viral protein(s), we used actinomycin D. Actinomycin D is known to lead to an inhibition of DNA synthesis and transcription. To inhibit cellular protein synthesis without affecting viral protein synthesis, Caco-2 cells were treated with 10 μg of actinomycin D/ml at time zero.

Antibodies and lectin. Rabbit polyclonal antirotavirus antibody 8148 was a gift from Jean Cohen. Tetramethyl rhodamine isothiocyanate (TRITC)-conjugated donkey anti-rabbit immunoglobulin G was purchased from Jackson Immuno-Research Laboratories via Interchim. Fluorescein isothiocyanate (FITC)-conjugated phalloidin was obtained from Molecular Probes via Interchim.

Immunofluorescence and confocal laser scanning microscopy (CLSM). Caco-2 cells cultured on coverslips were fixed with 2% paraformaldehyde for 15 min at room temperature, washed four times with phosphate-buffered saline containing 0.2% Tween 20 (PBS-Tween), and then permeabilized using Triton X-100. After three washes in PBS-Tween, cells were stained for F-actin or RRV by incubation with the antibodies or lectin described above for 60 min at room temperature. After four washes in PBS-Tween, incubation with TRITC-conjugated second antibody was performed for 1 h. Following four washes in PBS-Tween, cells were incubated for 10 min with DABCO antifading reagent and coverslips were mounted in Glycergel. Cells were observed in a Leitz Aristoplan microscope with epifluorescence or a Leica TCS equipped with a DMR inverted microscope and a 63/1.4 objective. A krypton-argon mixed-gas laser was used to generate two bands: 488 nm for FITC and 568 nm for TRITC. A band pass filter was used to recover FITC fluorescence, and an LP 590 filter was used for TRITC. Both fluorochromes were excited and analyzed in one pass with no interference between the two channels.

Statistical analysis. Values are given as means ± standard deviations. Statistical differences were determined by Student's *t* test.

RESULTS

Rotavirus infection induces $[Ca^{2+}]_i$ increase in Caco-2 cells. The intracellular calcium concentration was determined in Caco-2 cells infected with rotavirus RRV (Fig. 1A). In uninfected Caco-2 cells, the average basal $[Ca^{2+}]_i$ was 137 ± 8 nM ($n = 58$). In infected cells, a progressive increase in $[Ca^{2+}]_i$ from 7 h p.i. ($P < 0.01$) was measured. At 18 h p.i., $[Ca^{2+}]_i$ reached values on the order of 450 nM and was maintained at a steady state. No cell membrane alteration occurred at this time of infection, as indicated by evaluation of the LDH activity in culture supernatants (Fig. 1B). Measurements beyond 24 h were not reliable because of cell membrane alteration.

$[Ca^{2+}]_i$ increase induces microvillar F-actin disorganization in RRV-infected Caco-2 cells. As we have previously described (19), F-actin staining completely disappears from the brush border of RRV-infected cells at 24 h p.i. Here we observed that this microvillar F-actin disorganization could also be observed at 18 h p.i. (Fig. 2A to C) and coincided with the maximal value in $[Ca^{2+}]_i$ elevation, suggesting a possible relation between these two events. To determine the involvement of a $[Ca^{2+}]_i$ rise in microvillar actin alteration, we examined the effects of extra- and intracellular Ca^{2+} chelation on apical F-actin alteration in RRV-infected Caco-2 cells. Infected cells were treated at 15 h p.i. for 3 h with 3 mM EGTA to chelate extracellular Ca^{2+} and 75 μM BAPTA-AM to chelate intracellular Ca^{2+}. Virus replication in treated cells (6.90 ± 0.15, $n = 3$) was not significantly different ($P > 0.01$) from that observed in untreated cells (6.88 ± 0.02, $n = 3$). This treatment totally abolished the RRV-induced $[Ca^{2+}]_i$ rise (Fig. 2D) and RRV-induced microvillar actin alteration (Fig. 2E and F). These results suggest that a rotavirus-induced increase in

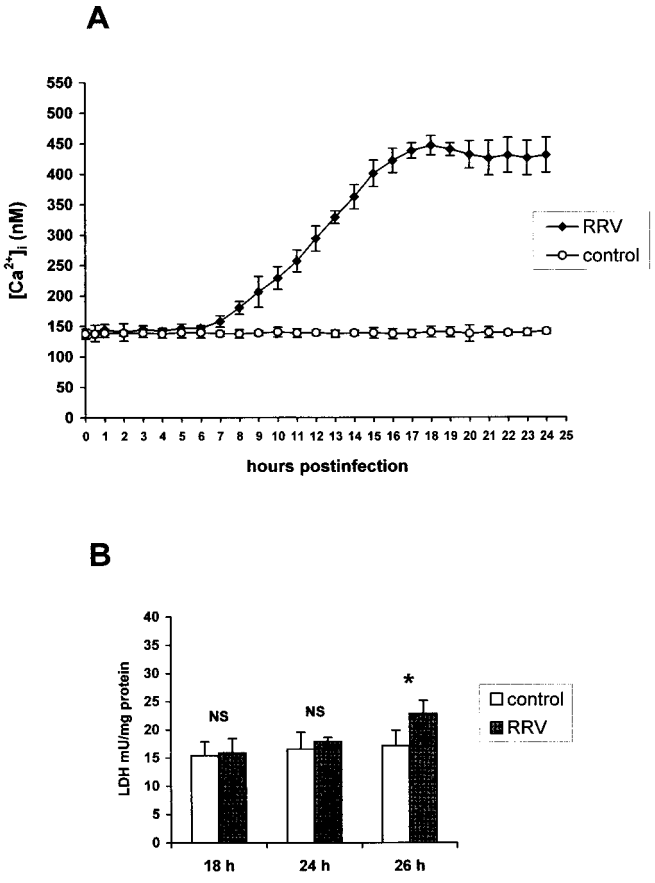

FIG. 1. (A) $[Ca^{2+}]_i$ in RRV-infected Caco-2 cells. Monolayers of 14- to 16-day-old Caco-2 cells were infected with RRV at an MOI of 10 PFU per cell and trypsinized at indicated times p.i. to measure $[Ca^{2+}]_i$ by quin2 fluorescence. Each point corresponds to the mean ± standard deviation of six independent measurements. (B) Time course of cell membrane integrity. Infected and mock-infected cells were assayed at indicated times p.i. for LDH release. Values are means ± standard deviations from 10 experiments. Statistical differences between control and infected cells were determined by Student's *t* test. NS, not significantly different; *, $P < 0.01$.

$[Ca^{2+}]_i$ is necessary for F-actin disorganization. To determine if the elevation in $[Ca^{2+}]_i$ was by itself responsible for apical actin alteration, mock-infected Caco-2 cells were treated with ionomycin, a Ca^{2+} ionophore. After 7 min of contact with 10 μM ionomycin, Caco-2 cells were fixed and permeabilized, and actin was stained with phalloidin-fluorescein. CLSM was used to study the spatial distribution of actin microfilaments. In ionomycin-treated cells, the F-actin staining completely disappeared from the apex of the cells (Fig. 2G). This alteration coincided with an elevation in $[Ca^{2+}]_i$ (data not shown) and was similar to that observed in 18 h p.i.-infected Caco-2 cells. Since ionomycin induces direct Ca^{2+} influx through the plasma membrane without involvement of other second messengers, we conclude that $[Ca^{2+}]_i$ increase is sufficient to induce microvillar actin alteration in Caco-2 cells.

Viral replication is necessary for $[Ca^{2+}]_i$ increase and microvillar cytoskeleton alteration. The relationships between viral protein synthesis and $[Ca^{2+}]_i$ elevation and between viral protein synthesis and microvillar F-actin alteration were studied using nonreplicating viral particles. The addition of nonreplicating viral particles to Caco-2 cells did not induce any change in $[Ca^{2+}]_i$, even after 18 h of contact (137 ± 8 nM for control cells, versus 138 ± 7 nM for cells incubated with non-

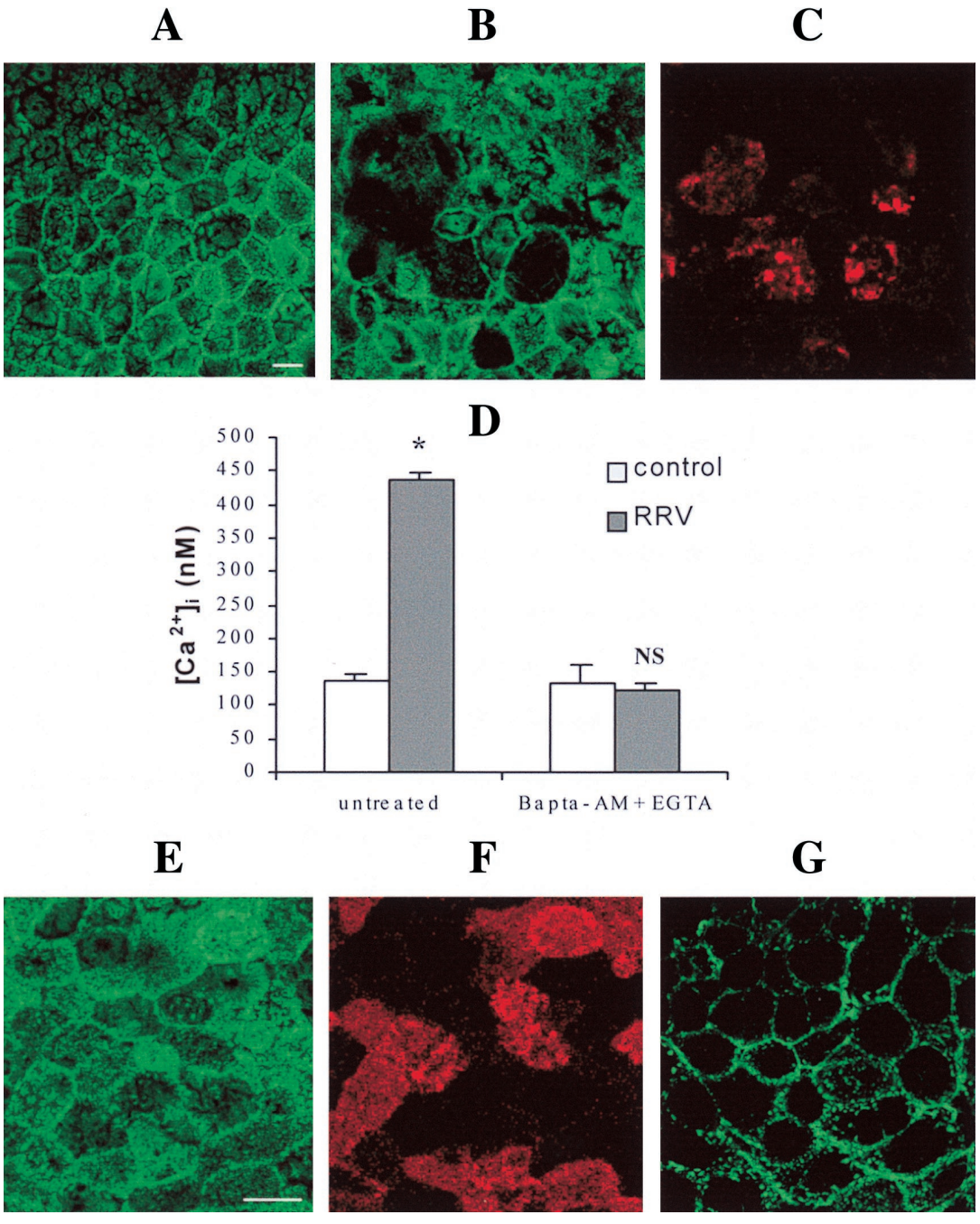

FIG. 2. Microvillar F-actin disassembly induced by RRV infection (A to C). At 18 h p.i., RRV-infected (B) and mock-infected (A) Caco-2 cells were fixed, permeabilized, and stained with fluorescein-phalloidin, which binds to F-actin. RRV proteins were immunostained with polyclonal anti-group A rotavirus antibody and rhodamine-labeled anti-rabbit immunoglobulin G antibody. A horizontal section was generated by CLSM at the apex of the cells. (C) RRV staining in the same cells as in panel B. Treatment of infected cells with EGTA and BAPTA-AM totally abolishes the RRV-induced $[Ca^{2+}]_i$ rise (D). Infected Caco-2 cells were treated at 15 h p.i. for 3 h with 3 mM EGTA and 75 μM BAPTA-AM. At 18 h p.i., cells were trypsinized to measure $[Ca^{2+}]_i$ by quin2 fluorescence. Values are means ± standard deviations from three experiments. Statistical differences between control and infected cells were determined by Student's *t* test. NS, not significantly different; ∗, $P < 0.01$. EGTA and BAPTA-AM treatment totally protects Caco-2 cells from RRV-induced microvillar F-actin alteration (E and F). (E) Microvillar F-actin staining in treated 18 h p.i.-infected cells; (F) RRV staining in the same cells as in panel E; (G) microvillar F-actin disorganization in Caco-2 cells stained with fluorescein-phalloidin after treatment for 7 min with 10 μM ionomycin. Bars, 10 μm.

replicating viral particles; $P > 0.01$). These results indicate that viral replication is necessary to induce a $[Ca^{2+}]_i$ increase in Caco-2 cells. Moreover, there was no alteration of brush border distribution of actin in Caco-2 cells in contact with inactivated RRV (data not shown). These results indicate that viral replication is also necessary to induce F-actin alteration in Caco-2 cells.

RRV infection of Caco-2 cells induces an increase in Ca^{2+} permeability of the plasma membrane. We next carried out

experiments to better understand the mechanisms responsible for the $[Ca^{2+}]_i$ increase in RRV-infected Caco-2 cells. $[Ca^{2+}]_i$ can be increased by different mechanisms. One possibility is that Ca^{2+} permeability of the plasma membrane is increased. This possibility was investigated by two means. First, we studied the effects of an increase in extracellular Ca^{2+} concentration on $[Ca^{2+}]_i$ in uninfected and infected cells (Fig. 3A). A step change in extracellular Ca^{2+} concentration induced an augmentation in quin2 fluorescence, the slope of which was higher in 18 h p.i.-infected cells. The fluorescence level attained was also much higher in RRV-infected cells than in control cells. The capacity of infected cells to recover the basal $[Ca^{2+}]_i$ level indicated that the mechanisms regulating cytosolic $[Ca^{2+}]_i$, such as ion pumps, were not inhibited. Second, we measured the Mn^{2+} influx in control and infected cells. As shown in Fig. 3C, the addition of Mn^{2+} to control cells induced a slight decrease of intracellular quin2 fluorescence due to the low resting permeability of the plasma membrane to divalent cations. In 18 h p.i.-infected cells, the rate of fluorescence quenching by Mn^{2+} was much faster than in mock-infected cells, and the level attained was much lower. Taken together, these two experimental approaches demonstrate that Ca^{2+} permeability of Caco-2 cells plasma membrane is increased as a result of rotavirus infection. A similar study was conducted with RRV-infected cells at 6 h p.i., before any increase in $[Ca^{2+}]_i$. In comparison with 18 h p.i., the same pattern of quenching was observed at 6 h p.i. but with a lower intensity (Fig. 3B). These data indicated that rotavirus infection induced an early modification in plasma membrane permeability.

Ca^{2+} accumulation in the internal stores in RRV-infected Caco-2 cells. $[Ca^{2+}]_i$ can also be raised by release of stored Ca^{2+} from the intracellular pools. The amount of total releasable Ca^{2+} was evaluated by measuring the elevation of $[Ca^{2+}]_i$ induced by 5 μM ionomycin in the absence of extracellular Ca^{2+}. Levels of Ca^{2+} released from the ionomycin-sensitive pool 2 min after suspension of the cells in Ca^{2+}-free EM containing 100 μM EGTA were 402 ± 54 nM in control cells, 537 ± 61 nM in 6 h p.i.-infected cells, and 554 ± 66 nM in 18 h p.i.-infected cells.

Ca^{2+} permeability of the internal store membranes increases at a late stage of RRV infection. To evaluate the permeability of the intracellular organelle membranes, Caco-2 cells were treated with 5 μM ionomycin 8 and 12 min after suspension in Ca^{2+}-free EM containing 100 μM EGTA. The rate of Ca^{2+} efflux from the intracellular compartments was quantified as the net change in $[Ca^{2+}]_i$ relative to the 2-min value (Fig. 4A). In RRV-infected cells at 18 h p.i., ionomycin-induced Ca^{2+} release decreased significantly faster ($P < 0.01$) compared with that in control cells: 12 min after suspension of the cells in Ca^{2+}-free EM, the average of ionomycin-induced Ca^{2+} release reached 46% of the 2-min level in RRV-infected cells, versus 82% in control cells ($P < 0.01$). In contrast, the percentage of ionomycin-induced Ca^{2+} release was not significantly different ($P > 0.01$) in RRV-infected at 12 h p.i. (78.11% ± 4.04%) compared with that in control cells. These results demonstrate that the permeability of the intracellular organelle membranes is not increased until 12 h p.i. In contrast, at a late stage of infection (e.g., 18 h p.i.), an efflux of Ca^{2+} from the intracellular organelles could be detected.

At a late stage of RRV infection, $[Ca^{2+}]_i$ rise in Caco-2 cells partially depends of Ca^{2+} mobilization from the ER. To determine if the ER Ca^{2+} stores were implicated in $[Ca^{2+}]_i$ elevation at a late stage of RRV infection, tBuBHQ, a specific inhibitor of the Ca^{2+}-ATPase pump localized in the ER membrane, was used. As shown in Fig. 4B, tBuBHQ treatment (50 μM) of 18 h p.i.-infected cells induced partial inhibition (about 40%) of the $[Ca^{2+}]_i$ rise measured at 18 h p.i. According to our previous results, no inhibition of $[Ca^{2+}]_i$ increase was measured in tBuBHQ-treated cells at 12 h p.i. These data suggest that from 18 h of infection, the rise in the $[Ca^{2+}]_i$ partially results from an increase in Ca^{2+} efflux from the ER.

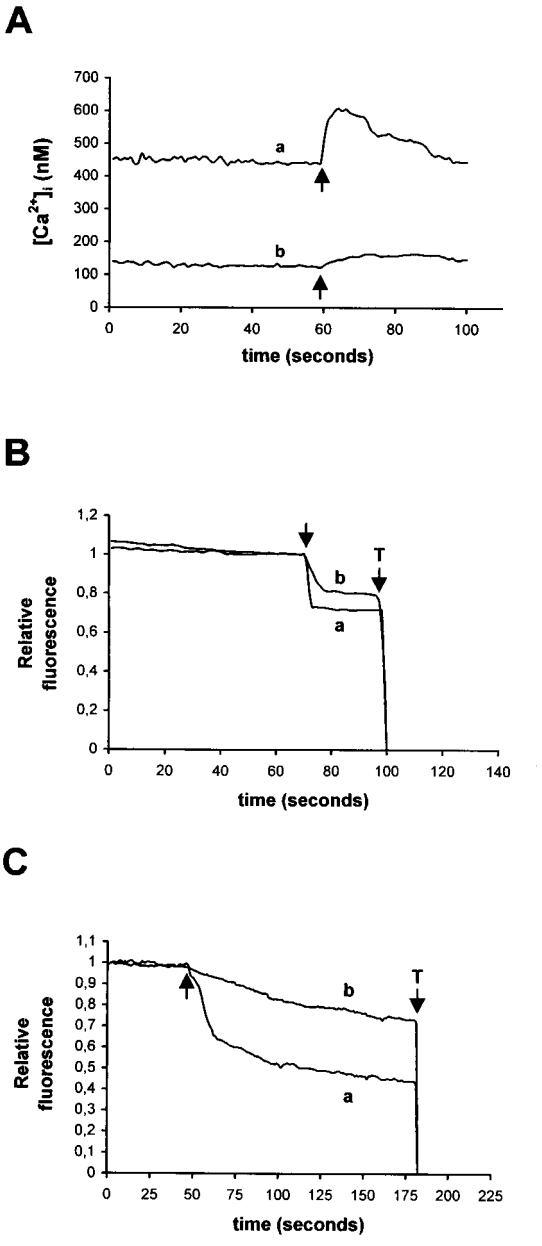

FIG. 3. Determination of plasma membrane permeability to Ca^{2+} in RRV-infected Caco-2 cells. At indicated times p.i., Caco-2 cells were trypsinized, and cell suspensions were loaded with quin2-AM for measurements of $[Ca^{2+}]_i$. (A) Evaluation of Ca^{2+} permeability of plasmalemma by the change in $[Ca^{2+}]_i$ induced by the addition of 5 mM $CaCl_2$ to the EM (arrows), which initially contained 1.8 mM Ca^{2+}, in 18 h p.i.-infected cells (a) and mock-infected cells (b). (B and C) Determination of plasmalemma permeability to Ca^{2+} by using Mn^{2+} as a substitute for Ca^{2+}. The quenching of quin2 fluorescence induced by addition of 0.5 mM Mn^{2+} (arrows) was measured at an excitation wavelength of 366 nm. Relative fluorescence corresponds to the normalized fluorescence, taking initial values as maximal and Triton X-100 (T) values as minimal. (B) Results for 6 h p.i.-infected (a) and mock-infected (b) cells; (C) 18 h p.i.-infected (a) and mock-infected (b) cells. Representative traces of series of 10 experiments are shown.

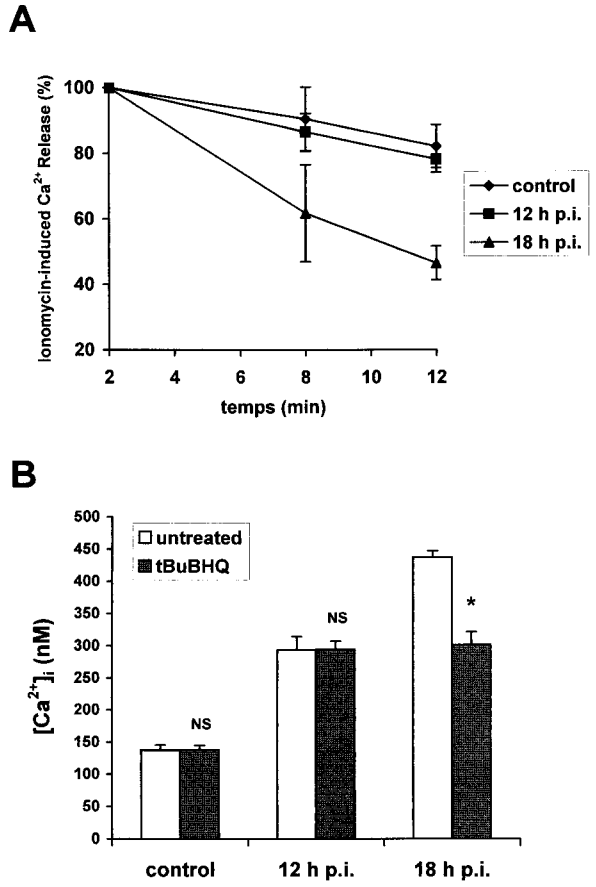

FIG. 4. Ca^{2+} release from the internal stores at a late stage of RRV infection of Caco-2 cells. (A) Ca^{2+} efflux from ionomycin-sensitive stores in RRV-infected Caco-2 cells at indicated times p.i. and in mock-infected cells. The peak change in $[Ca^{2+}]_i$ occurred following addition of ionomycin after 2, 8, and 12 min of suspension of quin2-AM-loaded cells in Ca^{2+}-free EM containing 100 μM EGTA. Each point represents mean ± standard deviation of the net change in $[Ca^{2+}]_i$ relative to the 2-min values from three independent experiments. (B) Effect of tBuBHQ on $[Ca^{2+}]_i$ increase induced by RRV infection of Caco-2 cells. tBuBHQ (50 μM) was added to Caco-2 cells 1 h before trypsinization and quin2-AM loading. $[Ca^{2+}]_i$ was measured in treated or untreated mock-infected and RRV-infected cells at indicated times p.i. Values are means ± standard deviations from six experiments. Statistical differences between untreated and tBuBHQ treated cells were determined by Student's *t* test. NS, not significantly different; *, $P < 0.01$.

$[Ca^{2+}]_i$ rise in RRV-infected Caco-2 cells partially depends on a PLC mechanism. To determine if the $[Ca^{2+}]_i$ increase was mediated by activation of a PLC pathway, the effects of RRV were examined in the presence of a PLC inhibitor, U-73122 (5). U-73343, a close analog of this molecule, has no inhibitory effect on PLC-dependent cellular signaling and was used as a control. U-73122 (50 μM) or U-73343 (50 μM) was added to infected Caco-2 cells at time zero, and $[Ca^{2+}]_i$ was measured at 12 or 18 h p.i. No effect of U-73122 was detected on $[Ca^{2+}]_i$ increase at 12 h p.i. However, $[Ca^{2+}]_i$ increase induced by RRV was partially (about 40%) inhibited in U-73122 treated cells at 18 h p.i. (Fig. 5). In contrast, U-73343 had no effect on $[Ca^{2+}]_i$ mobilization by RRV. The effect of U-73122 was not due to cellular toxicity since this agent did not affect $[Ca^{2+}]_i$ of noninfected Caco-2 cells. The effect of U-73122 was not due to inhibition of viral replication since viral production was not significantly different ($P > 0.01$) between U-73122 treated (7.71 ± 0.16, $n = 3$) and nontreated (7.69 ± 0.04, $n = 3$) cells. These results suggest that a PLC-dependent mechanism is

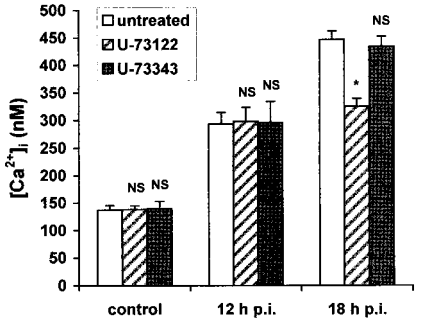

FIG. 5. At a late stage of RRV infection, $[Ca^{2+}]_i$ increase in Caco-2 cells partially depends on a PLC mechanism. U-73122, a PLC inhibitor, or U-73343, a close analog, was added to Caco-2 cells at time zero. Mock-infected and RRV-infected cells were trypsinized at indicated times p.i. to measure $[Ca^{2+}]_i$ by quin2 fluorescence. Values are means ± standard deviations from at least six experiments. Statistical differences between control and U-73122- or U-73343-treated cells were determined by Student's *t* test. NS, not significantly different; *, $P < 0.01$.

partially responsible for rotavirus-induced $[Ca^{2+}]_i$ increase, but only at a late stage of infection, from 18 h p.i.

Viral protein(s) released into supernatants of RRV-infected Caco-2 cells induce $[Ca^{2+}]_i$ increase in uninfected Caco-2 cells. To determine if viral components, present in culture supernatants of RRV-infected Caco-2 cells, induce alteration in Ca^{2+} homeostasis of Caco-2 cells, culture supernatants of RRV-infected cells were collected at different times p.i. and added to uninfected cells after quin2-AM loading. As shown in Fig. 6A, although $[Ca^{2+}]_i$ was not significantly modified by the treatment with supernatants of 12 h p.i.-infected cells ($P > 0.01$), a significant elevation in $[Ca^{2+}]_i$ could be measured when 15 h p.i.-infected cell supernatants were added ($P < 0.01$). After the addition of 18 to 24 h p.i.-infected cell supernatants, the $[Ca^{2+}]_i$ attained values 3.1 times higher than those in control cells. As shown in Fig. 6B, the increase in $[Ca^{2+}]_i$ induced by supernatants was transient and reached a maximal value after 22 min of incubation. These results indicate that late-stage culture supernatants of RRV-infected cells specifically induce a transient increase in $[Ca^{2+}]_i$ in Caco-2 cells. This effect was not due to the presence of viral particles in these supernatants. Indeed, when 10^7 to 10^9 RRV particles were added directly in the spectrofluorimeter cuvette to 2×10^6 quin2-AM-loaded uninfected Caco-2 cells, no increase in $[Ca^{2+}]_i$ was detected, even after 90 min of incubation (data not shown).

To determine if proteins were implicated in the $[Ca^{2+}]_i$ rise induced by RRV-infected cell supernatants, heated supernatants of infected Caco-2 cells were used. The addition of 18 h p.i.-heated supernatants did not induce any increase in $[Ca^{2+}]_i$ (Fig. 6B). To determine whether the $[Ca^{2+}]_i$ rise induced by supernatants was dependent on the synthesis of ex novo cell-coded proteins, $[Ca^{2+}]_i$ was measured after the addition of 18 h p.i.-infected supernatants from actinomycin D-treated cells. Treatment of RRV-infected cells with actinomycin D did not modify the ability of supernatants to induce $[Ca^{2+}]_i$ increase in mock-infected cells (Fig. 6C). These data suggest that the effects of supernatants of infected cells on $[Ca^{2+}]_i$ are related to the presence of one or several newly synthesized viral protein(s) or peptide(s).

To study the origin of the $[Ca^{2+}]_i$ rise induced by these RRV-secreted protein(s), we examined the effects of extracellular Ca^{2+} chelation on $[Ca^{2+}]_i$ elevation. Treatment of Caco-2 cells with 3 mM EGTA partially reduced the increase

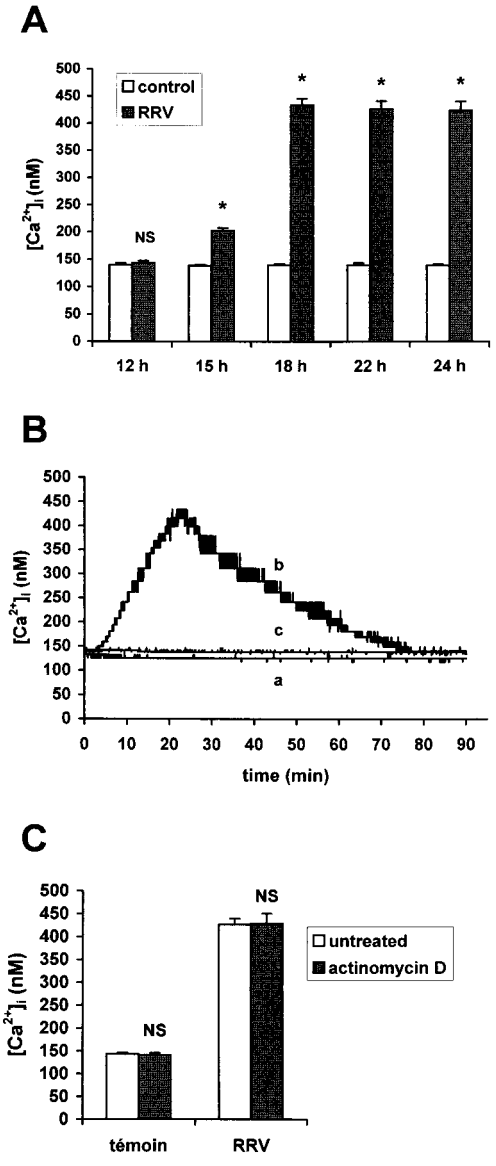

FIG. 6. Effect of culture supernatants of RRV-infected Caco-2 on $[Ca^{2+}]_i$ in uninfected Caco-2 cells. Caco-2 cells were infected with RRV at an MOI of 10 PFU/cell. (A) Peak values in $[Ca^{2+}]_i$ were measured after the addition to 2×10^6 quin2-AM loaded uninfected cells of supernatants of control or RRV-infected cells, collected at indicated times p.i. Values are means ± standard deviations from at least three to six experiments (see text). Statistical differences between peak values in $[Ca^{2+}]_i$ of infected and control cells were determined by Student's *t* test. NS, not significantly different; *, $P < 0.01$. (B) Effect of heated or nonheated 18 h p.i.-infected supernatants on $[Ca^{2+}]_i$ in uninfected Caco-2 cells. Supernatants of control cells (a), 18 h p.i.-infected cells (b), or 18 h p.i.-infected cells incubated at 95°C for 5 min (c) were added to uninfected Caco-2 cells immediately before $[Ca^{2+}]_i$ measurements. Representative traces from three to six independent experiments are shown. (C) Effect of actinomycin D on the increase in $[Ca^{2+}]_i$ induced by 18 h p.i.-infected cell supernatants. Supernatants issued from mock-infected or RRV-infected cells not treated or treated with actinomycin D (10 μg/ml) were added to quin2-loaded Caco-2 cells for $[Ca^{2+}]_i$ measurements. Values are means ± standard deviations from three experiments. Statistical differences between $[Ca^{2+}]_i$ of Caco-2 cells in the presence of treated and untreated supernatants were determined by Student's *t* test. NS, not significantly different.

in $[Ca^{2+}]_i$ (Fig. 7A), indicating that extracellular Ca^{2+} influx is not sufficient to explain the magnitude of $[Ca^{2+}]_i$ augmentation. To examine the possibility of a release of stored Ca^{2+} from the ER, Caco-2 cells were treated with 50 μM tBuBHQ.

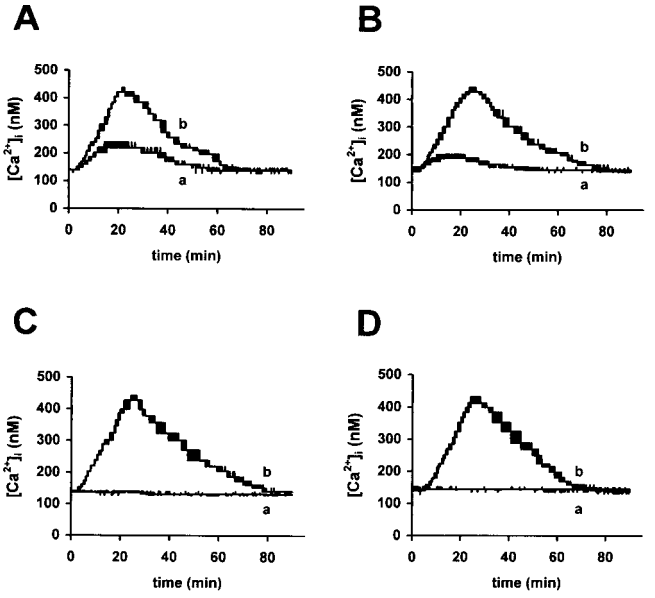

FIG. 7. Origin of the Ca^{2+} implicated in the $[Ca^{2+}]_i$ increase induced by supernatants of RRV-infected Caco-2 cells. (A) Quin2-AM loaded Caco-2 cells, not treated (b) or treated with 3 mM EGTA a few seconds before the addition of 18 h p.i.-infected supernatants (a); (B) Caco-2 cells, not treated (b) or treated with 50 μM tBuBHQ 10 min before the addition of 18 h p.i.-infected supernatants (a); (C) Caco-2 cells, not treated (b) or treated with 3 mM EGTA and 50 μM tBuBHQ before the addition of 18 h p.i.-infected supernatants (a); (D) Caco-2 cells, treated with 50 μM U-73122 (a) or 50 μM U-73343 (b) 10 min before the addition of 18 h p.i.-infected supernatants. Representative traces from three independent experiments are shown.

As shown in Fig. 7B, this treatment also induced partial inhibition of $[Ca^{2+}]_i$ elevation, indicating that part of $[Ca^{2+}]_i$ increase is due to the mobilization of Ca^{2+} from the ER. Simultaneous treatment of Caco-2 cells with 3 mM EGTA and 50 μM tBuBHQ totally abolished the increase in $[Ca^{2+}]_i$ (Fig. 7C). These results suggest that Ca^{2+} influx and Ca^{2+} mobilization from the ER are together responsible for the increase in $[Ca^{2+}]_i$ induced by RRV-secreted protein(s). Treatment of Caco-2 cells with 50 μM U-73122 10 min before the addition of supernatants of 18 h p.i.-infected cells totally abolished $[Ca^{2+}]_i$ increase (Fig. 7D). Since treatment with U-73343 did not modify $[Ca^{2+}]_i$ level, these results indicate that the effect of RRV-secreted protein(s) on Ca^{2+} homeostasis are mediated through a PLC-dependent mechanism.

Secreted viral protein(s) of 18 h p.i.-infected Caco-2 cell supernatants induces microvillar F-actin disorganization in Caco-2 cells. Since we have shown that $[Ca^{2+}]_i$ increase induces microvillar actin alteration in RRV-infected Caco-2 cells, we examined the effects of supernatants of RRV-infected cells on F-actin organization of uninfected Caco-2 cells. Cells were treated with 18 h p.i.-infected supernatants for indicated times, and F-actin was revealed as described above. After 40 min, marked alterations were observed in treated cells (Fig. 8B). F-actin staining disappeared from the apex of the cells and was detected only at the periphery of the cells. After 90 min, actin disorganization appeared to be completely reversed, as the cells presented a normal F-actin pattern (Fig. 8C). Treatment of Caco-2 cells with 50 μM tBuBHQ and 3 mM EGTA, which were shown to abolish the supernatant-induced $[Ca^{2+}]_i$ rise (see above), also prevented microvillar F-actin disorganization (Fig. 8D). Taken together, our results indicated that the transient increase in $[Ca^{2+}]_i$ induced by super-

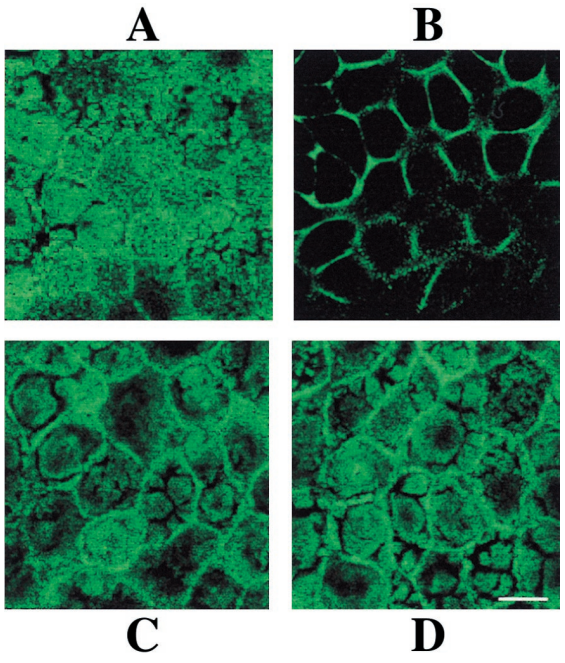

FIG. 8. Effect of supernatants of RRV-infected Caco-2 cells on microvillar F-actin organization of uninfected Caco-2 cells. At indicated times after the addition of 18 h p.i.-infected or mock-infected cell supernatants, Caco-2 cells were fixed, permeabilized, and stained with fluorescein-phalloidin. A horizontal section was generated by CLSM at the apex of the cells. F-actin staining 40 min after the addition of supernatants of mock-infected cells (A) or infected cells (B). (C) Normal F-actin pattern 90 min after the addition of supernatants of infected cells. Treatment of Caco-2 cells with 3 mM EGTA and 50 μM tBuBHQ (Fig. 7) prevented microvillar F-actin disorganization induced by supernatants of 18 h p.i.-infected cells (D). Bar, 10 μm.

natants of rotavirus-infected Caco-2 cells leads to a transient microvillar F-actin disassembly in mock-infected Caco-2 cells.

DISCUSSION

Our results demonstrate for the first time that rotavirus infection induces an increase in $[Ca^{2+}]_i$ in enterocyte-like cells that seems to be dependent on the synthesis of one or more viral and/or cellular component(s). We demonstrated that Ca^{2+} permeability of Caco-2 cell plasmalemma is increased during infection. It is of interest that in RRV-infected cells, after the elevation in $[Ca^{2+}]_i$ induced by a stepwise increase in the extracellular Ca^{2+}, return to the basal level was faster than in control cells. This observation seems to indicate that the mechanisms regulating $[Ca^{2+}]_i$ are not inhibited in RRV-infected Caco-2 cells. The activation of such regulatory mechanisms compensating for the increased Ca^{2+} entry may explain the absence of $[Ca^{2+}]_i$ elevation at 6 h p.i. The increase in Ca^{2+} in the intracellular organelles which we observed presumably corresponded to this activation of regulatory systems, such as Ca^{2+}-ATPase pumps of the ER. The comparison between the levels of plasma membrane permeability at 6 and 18 h p.i. indicates that the increase in Ca^{2+} permeability is higher as infection progresses. Therefore, after 6 h p.i., the progression in plasma membrane permeabilization beyond the capacity of the regulating systems seems to be responsible for the $[Ca^{2+}]_i$ increase. It is now well documented that elevated Ca^{2+} concentration in the ER is essential for rotavirus assembly and maturation (26, 31). Therefore, the Ca^{2+} concentration increase that we found in intracellular organelles of RRV-infected Caco-2 cells, including the ER, can be considered an essential step in rotavirus replication process.

We demonstrated that the ER Ca^{2+} pool is partially responsible for the $[Ca^{2+}]_i$ increase at a late stage of infection. It has been shown that depletion of Ca^{2+} from the ER can in turn induce extracellular Ca^{2+} influx in several types of cells (8, 11, 18, 23, 33). However, the increased Ca^{2+} influx that we observed in RRV-infected cells cannot be a secondary event due to the depletion of Ca^{2+} from the ER. Indeed, mobilization of Ca^{2+} from the ER appeared only at a late stage of infection, several hours after the increase in Ca^{2+} permeability of the plasmalemma. One possibility to explain the efflux of Ca^{2+} from the ER is the opening of preexisting Ca^{2+} channels. The opening of Ca^{2+} channels on the ER membrane is regulated by IP_3, produced by PLC which is usually activated by a surface receptor, often coupled to intracellular mediators through GTP-binding regulatory proteins (3). Since Ca^{2+} depletion of the ER induced by tBuBHQ is known to correspond to the mobilization of the IP_3-sensitive pool (22), the partial inhibition of $[Ca^{2+}]_i$ increase that we observed using this drug suggests an IP_3-dependent release of the ER Ca^{2+} stores during RRV infection. In accordance with these results, we demonstrated that at a late stage of infection, $[Ca^{2+}]_i$ is partially increased by a PLC-dependent Ca^{2+} release from the ER, through the opening of IP_3-sensitive channels. However, we cannot exclude the implication of other mechanisms facilitating the efflux of Ca^{2+}, such as a decreased pumping activity or a direct alteration of the ER membrane.

Taken together, these observations suggest that the mechanisms responsible for $[Ca^{2+}]_i$ increase in a monolayer of RRV-infected Caco-2 cells vary as a function of the stage of infection (Fig. 9). Based on our results, we propose that during the first hours of rotavirus infection, $[Ca^{2+}]_i$ elevation is due only to extracellular Ca^{2+} entry, resulting from the augmentation of plasma membrane permeability. At a late stage of infection (15 h p.i.), the increase in the Ca^{2+} permeability of the internal store membranes seems to be contradictory to the simultaneous accumulation of Ca^{2+} in the intracellular organelles of the same pool of cells. This contradiction could be explained by the existence of two types of cells at a late stage of infection: first, a pool of cells in which extracellular Ca^{2+} influx induces $[Ca^{2+}]_i$ elevation, as during the first hours of infection; and second, a pool of cells in which $[Ca^{2+}]_i$ increase partially or totally results from Ca^{2+} mobilization from the intracellular organelles, mainly the ER, probably through a PLC-dependent mechanism.

Since PLC is usually activated by a surface receptor, we investigated if supernatants of rotavirus-infected cells had the ability, through viral or cellular components, to induce $[Ca^{2+}]_i$ increase in Caco-2 cells. We showed that only supernatants of late stage-infected Caco-2 cells induce a rapid and transient increase in $[Ca^{2+}]_i$ of uninfected Caco-2 cells. Since we have shown that rotavirus did not induce any modification in $[Ca^{2+}]_i$ of Caco-2 cells without viral replication, the effect observed on $[Ca^{2+}]_i$ cannot be due to the direct interaction of rotavirus particles with Caco-2 cells. We demonstrated the proteinaceous nature of these components and the viral origin of these proteins or peptides. As the presence of these viral proteins in supernatants of infected cells is not related to cell lysis, our results suggest that the protein(s) or peptide(s) responsible for $[Ca^{2+}]_i$ transient increase is released from Caco-2 cells during the infectious process. Our study constitutes the first demonstration of alteration in Ca^{2+} homeostasis induced by viral proteins released into supernatants of rotavirus-infected cells. We determined that Ca^{2+} mobilization from the ER and extracellular Ca^{2+} influx into the cells are responsible for super-

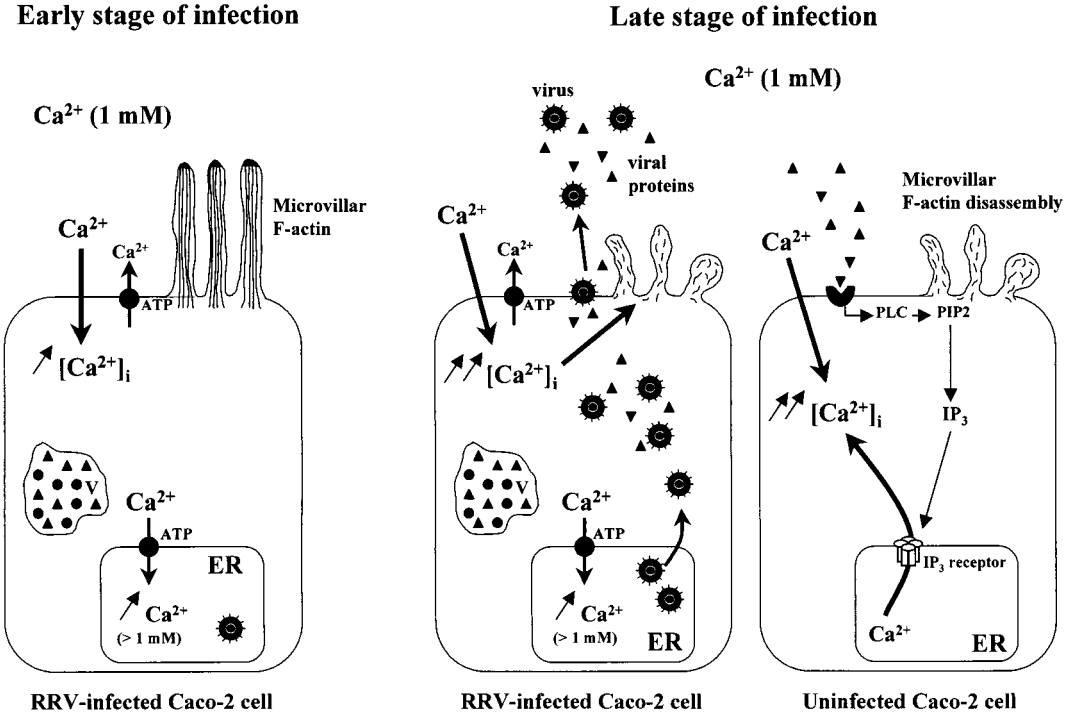

FIG. 9. A model depicting the mechanisms of $[Ca^{2+}]_i$ increase in a monolayer of RRV-infected Caco-2 cells as a function of the stage of infection. At an early stage of infection (from 7 to 12 h p.i.), $[Ca^{2+}]_i$ elevation is due only to extracellular Ca^{2+} entry and is partially compensated for by the activation of regulatory systems such as the Ca^{2+}-ATPase pump of the ER. At a late stage of infection, the $[Ca^{2+}]_i$ rise is more important in RRV-infected cells and induces microvillar F-actin disassembly from 18 h p.i. As of 15 h p.i., viral proteins or peptides released in extracellular medium from RRV-infected cells activate PLC in uninfected Caco-2 cells, through the interaction with a surface receptor. $[Ca^{2+}]_i$ increases by an IP_3-dependent mobilization of Ca^{2+} from the ER and by plasmalemma Ca^{2+} influx. This $[Ca^{2+}]_i$ rise also leads to microvillar F-actin disassembly. PIP2, phosphatidylinositol 4,5-biphosphate; V, viroplasm.

natant-induced $[Ca^{2+}]_i$ rise. This is not surprising, since as noted above, it has been shown that mobilization of Ca^{2+} from the ER can stimulate extracellular Ca^{2+} influx in mammalian cells. We (20) and others (34) have demonstrated that during RRV infection of Caco-2 cells at an MOI of 10, the proportion of infected cells after 18 h does not exceed 80%. Therefore, at a late stage of infection, uninfected cells can be stimulated for an increase in $[Ca^{2+}]_i$ by the viral proteins released in extracellular medium from RRV-infected Caco-2 cells (Fig. 9). Thus, they may constitute part of the pool of cells in which $[Ca^{2+}]_i$ is increased by a PLC-dependent mobilization of Ca^{2+} from the ER and plasmalemma Ca^{2+} influx. This could explain why in the late-stage-infected monolayer accumulation of Ca^{2+} in the internal stores could be detected simultaneously with efflux of Ca^{2+} from intracellular stores.

We determined that Ca^{2+} mobilization from the ER and Ca^{2+} influx are together responsible for viral secreted protein(s)-induced $[Ca^{2+}]_i$ increase through a PLC-dependent pathway. It has been reported that in Sf9 and HT29 clone 19A cells, the addition of 3 μM and 50 nM, respectively, viral glycoprotein NSP4 to the extracellular medium also induced a transient increase in $[Ca^{2+}]_i$ by a PLC-dependent mechanism (9, 35), through both Ca^{2+} release from intracellular stores and plasmalemma Ca^{2+} influx. Our results concerning the effect of secreted viral proteins on $[Ca^{2+}]_i$ are in complete accordance with these results. Indeed, Tian et al. have hypothesized (35) that at a late stage of infection, the NSP4 protein or fragments produced in rotavirus-infected cells could gain access to the extracellular medium and stimulate neighboring cells. Since our results indicate that viral protein(s) in late stage-supernatants of RRV-infected cells induces $[Ca^{2+}]_i$ increase in Caco-2 cells, it would be of interest to study the involvement of NSP4 in this process.

Since Ca^{2+} is known to be a determinant factor for actin cytoskeleton regulation, we studied the relationship between RRV-induced $[Ca^{2+}]_i$ rise and microvillar F-actin disassembly. We determined that the $[Ca^{2+}]_i$ rise triggered by RRV infection was directly responsible for changes in the organization of actin. Therefore, the $[Ca^{2+}]_i$ increase in rotavirus-infected intestinal epithelial cells could explain through F-actin disassembly the aberrantly shaped microvilli observed by electron microscopy (21), which could play a role in rotavirus pathogenesis by the reduction of the absorptive surface of the intestinal epithelium. We propose that the $[Ca^{2+}]_i$ increase may also be implicated in functional perturbations of rotavirus-infected intestinal epithelial cells, through structural alteration of the brush border. Indeed, in epithelial cells, the involvement of microvillar cytoskeleton in the organization of the apical pole is now well documented (1, 6, 14, 28, 32). Therefore, a $[Ca^{2+}]_i$ rise, through microvillar actin disassembly, may induce perturbations of the expression of intestinal hydrolases, such as SI, which leads to impaired nutrient digestion and thereby participates in triggering of diarrhea. Since we showed that the $[Ca^{2+}]_i$ increase induced by late-stage supernatants of RRV-infected cells induces a structural alteration in uninfected cells, F-actin disassembly may in turn be also responsible for functional perturbations in this type of cells. Taken together, our results are the first demonstration of the ability of one or several intracellular or released viral protein(s) from rotavirus-infected human intestinal epithelial cells to induce alteration in microvillar cytoskeleton, thereby participating in rotavirus pathogenesis. Therefore, this Ca^{2+}-dependent disorganization

of microvillar F-actin in enterocytes constitutes a new mechanism of rotavirus-induced cell injury, which may be implicated in triggering and/or amplification of diarrhea.

ACKNOWLEDGMENTS

This work was supported by a French Ministry of Research grant from the Réseau de Recherche sur les Gastro-entérites à Rotavirus: épidémiologie, structure et interaction avec l'hôte.

We thank J. Cohen (INRA, Jouy-en-Josas, France) for kindly providing antirotavirus serum and the RRV strain. We thank L. Combettes for helpful advice concerning intracellular calcium concentration measurements. Confocal experiments were performed with the kind cooperation of P. Fontanges and the Institut Fédératif de Recherche 65 INSERM.

REFERENCES

1. **Achler, C., D. Filmer, C. Merte, and D. Drenckhahn.** 1989. Role of microtubules in polarized delivery of apical membrane proteins to the brush border of the intestinal epithelium. J. Cell Biol. **109:**179–189.
2. **Ball, J. M., P. Tian, C. Q.-Y. Zeng, A. P. Morris, and M. K. Estes.** 1996. Age-dependent diarrhea induced by a rotaviral nonstructural glycoprotein. Science **272:**101–104.
3. **Berridge, M. J.** 1993. Inositol trisphosphate and calcium signalling. Nature **361:**315–325.
4. **Bishop, R. F., G. P. Davidson, I. H. Holmes, and B. J. Ruck.** 1973. Virus particles in epithelial cells of duodenal mucosa from children with acute non-bacterial gastroenteritis. Lancet **ii:**1281–1283.
5. **Bleasdale, J. E., N. R. Thakur, R. S. Gremban, G. L. Bundy, F. A. Fitzpatrick, R. J. Smith, and S. Bunting.** 1990. Selective inhibition of receptor-coupled phospholipase C-dependent processes in human platelets and polymorphonuclear neutrophils. J. Pharmacol. Exp. Ther. **255:**756–768.
6. **Costa de Beauregard, M.-A., E. Pringault, S. Robine, and D. Louvard.** 1995. Suppression of villin expression by antisense RNA impairs brush border assembly in polarized epithelial intestinal cells. EMBO J. **14:**409–421.
7. **Davidson, G. P., I. Goller, R. F. Bishop, R. R. W. Townley, I. H. Holmes, and B. J. Ruck.** 1975. Immunofluorescence in duodenal mucosa of children with acute enteritis due to a new virus. J. Clin. Pathol. **28:**263–266.
8. **Demerdash, T. M., N. Seyrek, M. Smogorzewski, W. Marcinkowski, S. Nasser-Moadelli, and S. G. Massry.** 1996. Pathways through which glucose induces a rise in $[Ca^{2+}]_i$ of polymorphonuclear leukocytes of rats. Kidney Int. **50:**2032–2040.
9. **Dong, Y., C. Q. Y. Zeng, J. M. Ball, M. K. Estes, and A. P. Morris.** 1997. The rotavirus enterotoxin NSP4 mobilizes intracellular calcium in human intestinal cells by stimulating phospholipase C-mediated inositol 1,4,5-trisphosphate production. Proc. Natl. Acad. Sci. USA **94:**3960–3965.
10. **Estes, M. K., and D. Y. Grahan.** 1980. Identification of rotaviruses of different origins by plaque reduction test. Am. J. Vet. Res. **41:**8–14.
11. **Foder, B., O. Scharff, and O. Thastrup.** 1989. Ca^{2+} transients and Mn^{2+} entry in human neutrophils induced by thapsigargin. Cell Calcium **10:**477–490.
12. **Fogh, J., J. M. Fogh, and T. Orfeo.** 1977. One hundred and twenty seven cultured human tumor cell lines producing tumor in nude mice. J. Natl. Cancer Inst. **59:**221–226.
13. **Friederich, E., E. Pringault, M. Arpin, and D. Louvard.** 1990. From the structure to the function of villin, an actin-binding protein of the brush border. Bioessays **12:**403–408.
14. **Gilbert, T., A. LeBivic, A. Quaroni, and E. Rodriguez-Boulan.** 1991. Microtubular organization and its involvement in the biogenetic pathways of plasma membrane proteins in Caco-2 intestinal epithelial cells. J. Cell Biol. **113:**275–288.
15. **Groene, W. S., and R. D. Shaw.** 1992. Psoralen preparation of antigenically intact noninfectious rotavirus particles. J. Virol. Methods **38:**93–102.
16. **Grynkiewicz, G., M. Poenie, and R. Y. Tsien.** 1985. A new generation of Ca^{2+} indicators with greatly improved fluorescence properties. J. Biol. Chem. **260:**3440–3450.
17. **Hassessian, H., L. Vaca, and D. L. Kunze.** 1994. Blockade of the inward rectifier potassium current by the Ca(2+)-ATPase inhibitor 2′,5′-di(tert-butyl)-1,4-benzohydroquinone (BHQ). Br. J. Pharmacol. **112:**1118–1122.
18. **Hu, Y., L. Vaca, X. Zhu, L. Birnbaumer, D. L. Kunze, and W. P. Schilling.** 1994. Appearance of a novel Ca^{2+} influx pathway in Sf9 insect cells following expression of the transient receptor potential-like (trpl) protein of Drosophila. Biochem. Biophys. Res. Commun. **201:**1050–1056.
19. **Jourdan, N., J.-P. Brunet, C. Sapin, A. Blais, J. Cotte-Laffitte, F. Forestier, A.-M. Quero, G. Trugnan, and A. Servin.** 1998. Rotavirus infection reduces sucrase-isomaltase expression in human intestinal epithelial cells by perturbing protein targeting and organization of microvillar cytoskeleton. J. Virol. **72:**7228–7236.
20. **Jourdan, N., J. Cotte-Laffitte, F. Forestier, A. L. Servin, and A. M. Quero.** 1995. Infection of cultured human intestinal cells by monkey RRV and human Wa rotavirus as a function of intestinal epithelial cell differentiation. Res. Virol. **146:**325–331.
21. **Jourdan, N., M. Maurice, D. Delautier, A. M. Quero, A. L. Servin, and G. Trugnan.** 1997. Rotavirus is released from the apical surface of cultured human intestinal cells through nonconventional vesicular transport that bypasses the Golgi apparatus. J. Virol. **71:**8268–8278.
22. **Kass, G. E., S. K. Duddy, G. A. Moore, and S. Orrenius.** 1989. 2,5-Di-(tert-butyl)-1,4-benzohydroquinone rapidly elevates cytosolic Ca^{2+} concentration by mobilizing the inositol 1,4,5-trisphosphate-sensitive Ca^{2+} pool. J. Biol. Chem. **264:**15192–15198.
23. **Keay, S., B. R. Baldwin, M. W. Smith, S. S. Wasserman, and W. F. Goldman.** 1995. Increases in $[Ca^{2+}]_i$ mediated by the 92.5-kDa putative cell membrane receptor for HCMV gp86. Am. J. Physiol. **269:**C11–C21.
24. **Merritt, J. E., R. Jacob, and T. J. Hallam.** 1989. Use of manganese to discriminate between calcium influx and mobilization from internal stores in stimulated human neutrophils. J. Biol. Chem. **264:**1522–1527.
25. **Mertz, L. M., B. J. Baum, and I. S. Ambudkar.** 1990. Refill status of the agonist-sensitive Ca^{2+} pool regulates Mn^{2+} influx into parotid acini. J. Biol. Chem. **265:**15010–15014.
26. **Michelangeli, F., F. Liprandi, M. E. Chemello, M. Ciarlet, and M.-C. Ruiz.** 1995. Selective depletion of stored calcium by thapsigargin blocks rotavirus maturation but not the cytopathic effect. J. Virol. **69:**3838–3847.
27. **Michelangeli, F., M.-C. Ruiz, J. R. Del Castillo, J. E. Ludert, and F. Liprandi.** 1991. Effect of rotavirus infection on intracellular calcium homeostasis in cultured cells. Virology **181:**520–527.
28. **Ojakian, G. K., and R. Schwimmer.** 1988. The polarized distribution of an apical cell surface glycoprotein is maintained by interactions with the cytoskeleton of Madin-Darby canine kidney cells. J. Cell Biol. **107:**2377–2387.
29. **Perez, J. F., M. E. Chemello, F. Liprandi, M. C. Ruiz, and F. Michelangeli.** 1998. Oncosis in MA104 cells is induced by rotavirus infection through an increase in intracellular Ca^{2+} concentration. Virology **252:**17–27.
30. **Pinto, M., S. Robine-Leon, M. D. Appay, M. Kedinger, N. Triadou, E. Dussaulx, B. Lacroix, P. Simon-Assman, K. Haffen, J. Fogh, and A. Zweibaum.** 1983. Enterocyte-like differentiation and polarization of the human colon carcinoma cell line Caco-2 in culture. Biol. Cell **47:**323–330.
31. **Poruchynsky, M. S., D. R. Maass, and P. H. Atkinson.** 1991. Calcium depletion blocks the maturation of rotavirus by altering the oligomerization of virus-encoded proteins in the ER. J. Cell Biol. **114:**4.
32. **Salas, P. J. I., M. L. Rodriguez, A. L. Viciana, D. E. Vegas-Salas, and H. P. Hauri.** 1997. The apical submembrane cytoskeleton participate in the organization of the apical pole in epithelial cells. J. Cell Biol. **137:**359–375.
33. **Schilling, W. P., L. Rajan, and E. Strobl-Jager.** 1989. Characterization of the bradykinin-stimulated calcium influx pathway of cultured vascular endothelial cells. Saturability, selectivity, and kinetics. J. Biol. Chem. **264:**12838–12848.
34. **Svensson, L., B. B. Finlay, D. Bass, C. H. vonBonsdorff, and H. B. Greenberg.** 1991. Symmetric infection of rotavirus on polarized human intestinal epithelial (Caco-2) cells. J. Virol. **65:**4190–4197.
35. **Tian, P., M. K. Estes, Y. Hu, J. M. Ball, C. Q. Y. Zeng, and W. P. Schilling.** 1995. The rotavirus nonstructural glycoprotein NSP4 mobilizes Ca^{2+} from the endoplasmic reticulum. J. Virol. **69:**5763–5772.
36. **Tian, P., Y. Hu, W. P. Shilling, D. A. Lindsay, J. Eiden, and M. K. Estes.** 1994. The nonstructural glycoprotein of rotavirus affects intracellular calcium levels. J. Virol. **68:**251–257.
37. **Tsien, R. Y., T. Pozzan, and T. J. Rink.** 1982. Calcium homeostasis in intact lymphocytes: cytoplasmic free calcium monitored with a new, intracellularly trapped fluorescent indicator. J. Cell Biol. **94:**325–334.
38. **Weeds, A., and S. Maciver.** 1993. F-actin capping proteins. Curr. Opin. Cell Biol. **5:**63–69.
39. **Zweibaum, A., M. Laburthe, E. Grasset, and D. Louvard.** 1991. Use of cultured cell lines in studies of intestinal cell differentiation and function, p. 223–255. *In* S. J. Schultz, M. Field, and R. A. Frizell (ed.), Handbook of physiology. The Gastrointestinal System, vol. IV. Intestinal absorption and secretion. American Physiological Society, Bethesda, Md.